Andreev Reflection

Fabrizio Dolcini
Scuola Normale Superiore di Pisa, NEST (Italy)
Dipartimento di Fisica del Politecnico di Torino (Italy)

Lecture Notes for XXIII Physics GradDays, Heidelberg, 5-9 October 2009

Contents

Chapter 1

Andreev Reflection

1.1 The Blonder-Tinkham-Klapwijk model for N-S junction

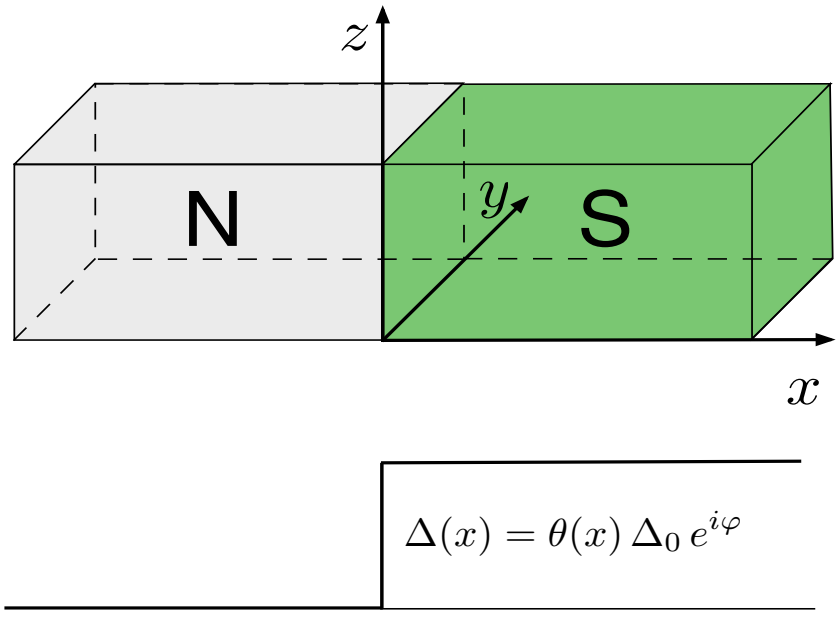

Figure 1.1: Scheme of a N-S junction.

- Let us consider a normal(N) - superconductor(S) junction, as shown in Fig.1.1. We denote by x the longitudinal coordinate and by (y, z) the transversal coordinates. The junction is located at the coordinate $x = 0$. We model the system with the Bogolubov de Gennes Equation

$$\begin{pmatrix} \mathcal{H}_e & \Delta \\ \Delta^* & -\mathcal{H}_e^* \end{pmatrix} \begin{pmatrix} u \\ v \end{pmatrix} = E \begin{pmatrix} u \\ v \end{pmatrix} \tag{1.1}$$

- We describe the junction with a step-like order parameter

$$\Delta(x) = \theta(x)\,\Delta_0\,e^{i\varphi} \tag{1.2}$$

- Assume that the system is separable, so that
  i) we can factorize the wavefunction into

$$\Psi(x,y,z) = \psi(x)\,\Phi_n(y,z) \qquad \begin{cases} \psi(x) & = & \text{longitudinal wavefunction} \\ \Phi_n(y,z) & = & \text{transversal wavefunction} \end{cases} \tag{1.3}$$

  where n denotes the quantum number labeling the transversal mode

$$\left[-\frac{\hbar^2}{2m}\left(\frac{\partial^2}{\partial x^2}+\frac{\partial^2}{\partial y^2}\right)+V_\perp(y,z)\right]\Phi_n(y,z) = E_n\Phi_n(y,z) \tag{1.4}$$

  with transversal energy E_n, and $V_\perp$ is the transversal confining potential.

  ii) The energy is the sum of the longitudinal and transversal energies

$$E = E_{//} + E_n \tag{1.5}$$

  so that, for a given transversal mode n, the effective chemical potential for the longitudinal propagation reads

$$\varepsilon_{Fn} = \varepsilon_F - E_n \tag{1.6}$$

  where we assume that ε_F already includes the self-consistent potential U.

- We include a $\Lambda\delta(x)$ potential at the boundary in order to account for the contact resistance of the interface.

In conclusion, the system is described by the following effective 1D BdG Hamiltonian

$$\boxed{\begin{pmatrix} -\frac{\hbar^2}{2m}\frac{\partial^2}{\partial x^2} - \varepsilon_{Fn} + \Lambda\delta(x) & \Delta(x) \\ \Delta^*(x) & \frac{\hbar^2}{2m}\frac{\partial^2}{\partial x^2} + \varepsilon_{Fn} - \Lambda\delta(x) \end{pmatrix}\begin{pmatrix} u(x) \\ v(x) \end{pmatrix} = E\begin{pmatrix} u(x) \\ v(x) \end{pmatrix}} \tag{1.7}$$

and is called the **Blonder-Tinkham-Klapwijk (BTK) Model**, as described in Ref.[7]. The purpose is thus to find solutions with non negative energy $E \geq 0$.

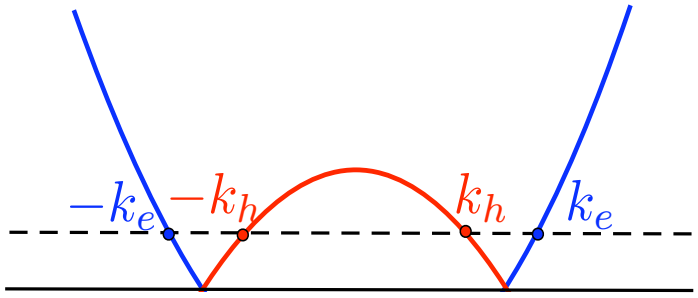

Figure 1.2: Spectrum in the N region.

1.2 Solutions in N

In the normal side N the equation (1.7) reduces to

$$\begin{pmatrix} -\frac{\hbar^2}{2m}\frac{\partial^2}{\partial x^2} - \varepsilon_{Fn} & 0 \\ 0 & \frac{\hbar^2}{2m}\frac{\partial^2}{\partial x^2} + \varepsilon_{Fn} \end{pmatrix} \begin{pmatrix} u(x) \\ v(x) \end{pmatrix} = E \begin{pmatrix} u(x) \\ v(x) \end{pmatrix} \tag{1.8}$$

which exhibits two particle solutions

$$\Psi^e_{\pm}(x) = \begin{pmatrix} 1 \\ 0 \end{pmatrix} e^{\pm i k_e x} \tag{1.9}$$

and two hole solutions

$$\Psi^h_{\pm}(x) = \begin{pmatrix} 0 \\ 1 \end{pmatrix} e^{\pm i k_h x} \tag{1.10}$$

where

$$k_e = k_{Fn}\sqrt{1 + \frac{E}{\varepsilon_{Fn}}} \tag{1.11}$$

$$k_h = k_{Fn}\sqrt{1 - \frac{E}{\varepsilon_{Fn}}} \tag{1.12}$$

and

$$k_{Fn} = \frac{\sqrt{2m\varepsilon_{Fn}}}{\hbar} \tag{1.13}$$

1.3 Solutions in S

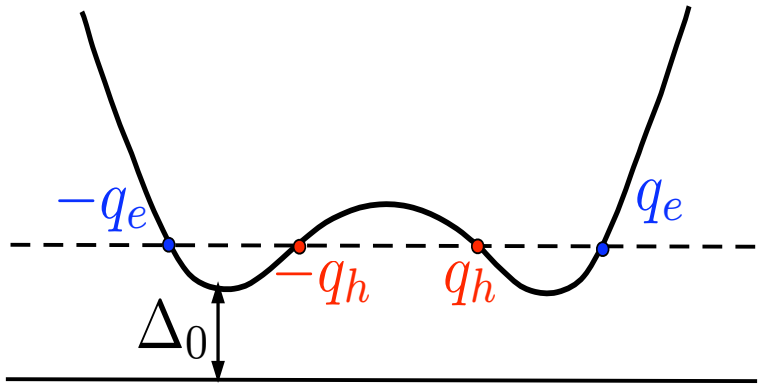

Figure 1.3: Spectrum in the S region.

In the superconductor side S the equation (1.7) reduces to

$$\begin{pmatrix} -\frac{\hbar^2}{2m}\frac{\partial^2}{\partial x^2} - \varepsilon_{Fn} & \Delta_0\, e^{i\varphi} \\ \Delta_0\, e^{-i\varphi} & \frac{\hbar^2}{2m}\frac{\partial^2}{\partial x^2} + \varepsilon_{Fn} \end{pmatrix} \begin{pmatrix} u(x) \\ v(x) \end{pmatrix} = E \begin{pmatrix} u(x) \\ v(x) \end{pmatrix} \tag{1.14}$$

We have to distinguish two cases

1.3.1 Supra-gap solutions ($E > \Delta_0$): propagating waves

Here there are two particle-like solutions

$$\Psi^e_\pm(x) = \begin{pmatrix} u_0\, e^{i\varphi/2} \\ v_0\, e^{-i\varphi/2} \end{pmatrix} e^{\pm i q_e x} \tag{1.15}$$

and two hole-like solutions

$$\Psi^h_\pm(x) = \begin{pmatrix} v_0\, e^{i\varphi/2} \\ u_0\, e^{-i\varphi/2} \end{pmatrix} e^{\pm i q_h x} \tag{1.16}$$

where

$$q_e = k_{Fn}\sqrt{1 + \sqrt{\frac{E^2 - \Delta_0^2}{\varepsilon_{Fn}^2}}} \tag{1.17}$$

$$q_h = k_{Fn}\sqrt{1 - \sqrt{\frac{E^2 - \Delta_0^2}{\varepsilon_{Fn}^2}}} \tag{1.18}$$

and

$$k_{Fn} = \frac{\sqrt{2m\varepsilon_{Fn}}}{\hbar} \tag{1.19}$$

Here, the quantities u_0 and v_0 read

$$u_0 = \sqrt{\frac{1}{2}\left(1+\sqrt{1-\left(\frac{\Delta_0}{E}\right)^2}\right)} \equiv \sqrt{\frac{\Delta_0}{2E}}\, e^{\frac{1}{2}\mathrm{arccosh}\frac{E}{\Delta_0}} \tag{1.20}$$

$$v_0 = \sqrt{\frac{1}{2}\left(1-\sqrt{1-\left(\frac{\Delta_0}{E}\right)^2}\right)} \equiv \sqrt{\frac{\Delta_0}{2E}}\, e^{-\frac{1}{2}\mathrm{arccosh}\frac{E}{\Delta_0}} \tag{1.21}$$

so that the wavefunctions (1.15) and (1.16)

$$\Psi^e_{\pm}(x) = \sqrt{\frac{\Delta_0}{2E}} \begin{pmatrix} e^{\frac{1}{2}\mathrm{arccosh}\frac{E}{\Delta_0}}\, e^{i\varphi/2} \\ \\ e^{-\frac{1}{2}\mathrm{arccosh}\frac{E}{\Delta_0}}\, e^{-i\varphi/2} \end{pmatrix} e^{\pm iq_e x} \tag{1.22}$$

and two hole-like solutions

$$\Psi^h_{\pm}(x) = \sqrt{\frac{\Delta_0}{2E}} \begin{pmatrix} e^{-\frac{1}{2}\mathrm{arccosh}\frac{E}{\Delta_0}}\, e^{i\varphi/2} \\ \\ e^{\frac{1}{2}\mathrm{arccosh}\frac{E}{\Delta_0}}\, e^{-i\varphi/2} \end{pmatrix} e^{\pm iq_h x} \tag{1.23}$$

1.3.2 Sub-gap solutions ($E < \Delta_0$): evanescent waves

In the subgap solutions $q_{e/h}$ acquire an imaginary part. A real part remains and is of the order of k_{Fn}. The solution is the analytic continuation of (1.24) and (1.25), and reads

$$q_e = k_{Fn}\sqrt{1+i\sqrt{\frac{\Delta_0^2-E^2}{\varepsilon_{Fn}^2}}} \tag{1.24}$$

$$q_h = k_{Fn}\sqrt{1-i\sqrt{\frac{\Delta_0^2-E^2}{\varepsilon_{Fn}^2}}} \tag{1.25}$$

Similarly the analytic continuation of (1.20) and (1.21) reads

$$u_0 = \sqrt{\frac{\Delta_0}{2E}}\, e^{\frac{i}{2}\arccos\frac{E}{\Delta_0}} \tag{1.26}$$

$$v_0 = \sqrt{\frac{\Delta_0}{2E}}\, e^{-\frac{i}{2}\arccos\frac{E}{\Delta_0}} \tag{1.27}$$

Remark
Notice that for the evanescent waves one has $|u_0|^2 + |v_0|^2 \neq 1$. Instead one has

$$\begin{aligned} u_0^2 + v_0^2 &= \frac{\Delta_0}{2E}\left(e^{i\arccos\frac{E}{\Delta_0}} + e^{-i\arccos\frac{E}{\Delta_0}}\right) = \\ &= \frac{\Delta_0}{2E}\,2\cos\left(\arccos\frac{E}{\Delta_0}\right) = 1 \end{aligned} \tag{1.28}$$

Analytic continuation is important because we know from causality that S-matrix in the supra-gap regime admits an analytic continuation into the sub-gap regime. Such continuation is in general not unitary. Unitarity only holds for propagating modes, because evanescent waves carry no current and unitarity is related to the conservation of current.

1.4 Condition at the boundary

Integrating the equation

$$-\frac{\hbar^2}{2m}\frac{\partial^2 u}{\partial x^2} - \varepsilon_{Fn}u(x) + \Lambda\delta(x)u(x) + \Delta(x)v(x) = Eu(x)$$

around $x = 0$, one obtains the boundary conditions for the derivatives

$$\boxed{\partial_x u(0^+) - \partial_x u(0^-) = \frac{2m\Lambda}{\hbar^2}\,u(0)} \tag{1.29}$$

and

$$\boxed{\partial_x v(0^+) - \partial_x v(0^-) = \frac{2m\Lambda}{\hbar^2}\,v(0)} \tag{1.30}$$

1.5 Scattering Matrix Coefficient

We now want to determine the coefficient of the Scattering Matrix. Let us start by considering the case of an incident electron, incoming from the N left electrode towards the interface

$$\Psi_{in}(x) = \frac{1}{\sqrt{2\pi\hbar v_e}}\begin{pmatrix}1\\0\end{pmatrix} e^{+ik_e x} \tag{1.31}$$

The wave reflected back into the N region is a left-moving electron or a left-moving hole, i.e.

$$\Psi_{refl}(x) = \frac{r_{ee}}{\sqrt{2\pi\hbar v_e}}\begin{pmatrix}1\\0\end{pmatrix} e^{-ik_e x} + \frac{r_{he}}{\sqrt{2\pi\hbar v_h}}\begin{pmatrix}0\\1\end{pmatrix} e^{+ik_h x} \tag{1.32}$$

In contrast, the transmitted wave is a right-moving electron-like or a right-moving hole-like solution

$$\Psi_{trans}(x) = \frac{t_{ee}}{\sqrt{2\pi\hbar\, w_e}}\begin{pmatrix}u_0\, e^{i\varphi/2}\\ v_0\, e^{-i\varphi/2}\end{pmatrix} e^{+iq_e x} + \frac{t_{he}}{\sqrt{2\pi\hbar\, w_h}}\begin{pmatrix}v_0\, e^{i\varphi/2}\\ u_0\, e^{-i\varphi/2}\end{pmatrix} e^{-iq_h x} \tag{1.33}$$

Remarks

- We have denoted

$$r_{ee} = \text{reflection coefficient} \quad \text{e} \to \text{e} \tag{1.34}$$
$$r_{he} = \text{reflection coefficient} \quad \text{e} \to \text{h} \tag{1.35}$$
$$t_{ee} = \text{transmission coefficient} \quad \text{e} \to \text{e} \tag{1.36}$$
$$t_{he} = \text{transmission coefficient} \quad \text{e} \to \text{h} \tag{1.37}$$

- We have normalized the wavefunctions with their velocities, because they are different in general for particle and holes, and from normal to superconduting side. In this way, each wavefunction carries the same amount of flux of quasiparticle probability current[4], and therefore the above coefficients describe a unitary matrix. We recall that unitarity of the scattering matrix stems from the conservation of quasi-particle probability current.
  For the N side we have

$$E = \frac{\hbar^2 k_e^2}{2m} - \varepsilon_{Fn} \qquad \Rightarrow \qquad v_e = \frac{1}{\hbar}\left|\frac{dE}{dk_e}\right| = \frac{\hbar k_e}{m} \tag{1.38}$$
$$E = \varepsilon_{Fn} - \frac{\hbar^2 k_h^2}{2m} \qquad \Rightarrow \qquad v_h = \frac{1}{\hbar}\left|\frac{dE}{dk_h}\right| = \frac{\hbar k_h}{m} \tag{1.39}$$

  For the S side we have

$$E = \sqrt{\left(\frac{\hbar^2 q_e^2}{2m} - \varepsilon_{Fn}\right)^2 + \Delta_0^2} \qquad \Rightarrow \qquad w_e = \frac{1}{\hbar}\left|\frac{dE}{dq_e}\right| = \frac{\hbar q_e}{m} \tag{1.40}$$
$$E = \sqrt{\left(\varepsilon_{Fn} - \frac{\hbar^2 q_h^2}{2m}\right)^2 + \Delta_0^2} \qquad \Rightarrow \qquad w_h = \frac{1}{\hbar}\left|\frac{dE}{dq_h}\right| = \frac{\hbar q_h}{m} \tag{1.41}$$

  The velocities are

$$v_{e/h} = \frac{\hbar k_{e/h}}{m} \tag{1.42}$$
$$w_{e/h} = \frac{\sqrt{E^2 - \Delta_0^2}}{E}\, v_{e/h} = (u_0^2 - v_0^2) v_{e/h} \tag{1.43}$$

- In the reflected wave the momenta of the electron and hole have opposite signs, just because we want to describe left-moving waves. Similarly for the right-moving transmitted waves (see Fig.1.4).

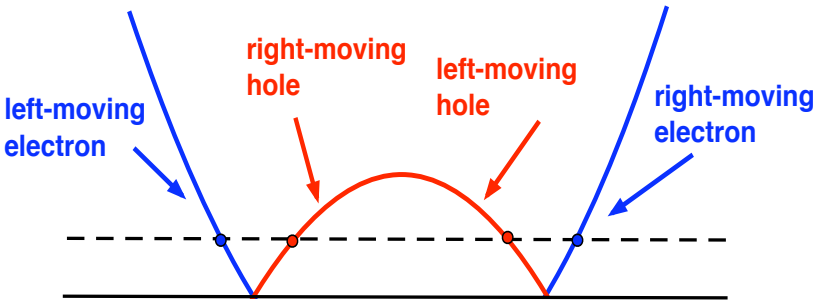

Figure 1.4: Different signs of velocities in the electron-hole band.

In order to find the solution we have to impose

$$u(0^+) = u(0^-) \qquad \text{(continuity)} \tag{1.44}$$

$$v(0^+) = v(0^-) \qquad \text{(continuity)} \tag{1.45}$$

$$\tag{1.46}$$

$$\partial_x u(0^+) - \partial_x u(0^-) = \frac{2m\Lambda}{\hbar^2}\, u(0) \qquad \text{(derivative)} \tag{1.47}$$

$$\partial_x v(0^+) - \partial_x v(0^-) = \frac{2m\Lambda}{\hbar^2}\, v(0) \qquad \text{(derivative)} \tag{1.48}$$

These conditions represent a set of four linear equations for the four unknowns r_{ee}, r_{he}, t_{ee}, and t_{he}.

Exploiting the linearity of the above equations, one can find the other scattering matrix coefficients (such as r_{eh}, t_{eh} and so on) by setting *e.g.* an incoming hole from N or incoming electron/hole from S, and superimposing the various solutions.

1.6 Solution in the Andreev Approximation

The explicit solution of the linear set of equation is particularly simple in the so called Andreev approximation, which consists in envisaging low energies with respect to the Fermi level

$$E, \Delta_0 \ll \varepsilon_{Fn} \tag{1.49}$$

and thus retain the lowest order in E/ε_{Fn} and $\Delta_0/\varepsilon_{Fn}$. One can then approximate

$$k_{e/h} \simeq q_{e/h} \simeq k_{Fn} \tag{1.50}$$

and

$$v_{e/h} \simeq v_{Fn} \tag{1.51}$$

$$w_{e/h} \simeq \frac{\sqrt{E^2 - \Delta_0^2}}{E}\, v_{Fn} = (u_0^2 - v_0^2)\, v_{Fn} \tag{1.52}$$

with the Fermi velocity defined as

$$v_{Fn} = \frac{\hbar k_{Fn}}{m} \tag{1.53}$$

Under the Andreev approximation one finds

- for the transmission and reflection amplitudes

$$r_{he} = \frac{u_0 v_0}{u_0^2 + Z^2(u_0^2 - v_0^2)}\, e^{-i\varphi} \tag{1.54}$$

$$r_{ee} = \frac{(Z^2 + iZ)(v_0^2 - u_0^2)}{u_0^2 + Z^2(u_0^2 - v_0^2)} \tag{1.55}$$

$$t_{ee} = \frac{(1 - iZ)u_0\sqrt{u_0^2 - v_0^2}}{u_0^2 + Z^2(u_0^2 - v_0^2)}\, e^{-i\varphi/2} \tag{1.56}$$

$$t_{he} = \frac{iZv_0\sqrt{u_0^2 - v_0^2}}{u_0^2 + Z^2(u_0^2 - v_0^2)}\, e^{-i\varphi/2} \tag{1.57}$$

Here

$$Z = \frac{\Lambda m}{\hbar^2 k_{Fn}} = \frac{\Lambda}{\hbar v_{Fn}} \tag{1.58}$$

is the BTK dimensionless parameter of the interface transparency

$$\begin{cases} Z \ll 1 & \text{very transparent interface} \\ \\ Z \gg 1 & \text{weakly transparent interface (tunnel limit)} \end{cases} \tag{1.59}$$

By the transparency we mean the transmission probability T_N of the junction *in the normal case*, i.e. when the gap in the superconducting side is set to zero ($\Delta_0 \to 0$) or the temperature is above the critical temperature T_c. One can prove that the BTK parameter is related to T_N through the relation

$$T_N = \frac{1}{1 + Z^2} \tag{1.60}$$

- The corresponding transmission and reflection coefficients read

$$A \doteq A_{LL}^{he} \doteq |r_{he}|^2 \tag{1.61}$$

$$B \doteq A_{LL}^{ee} \doteq |r_{ee}|^2 \tag{1.62}$$

$$C \doteq A_{RL}^{ee} \doteq |t_{ee}|^2 \tag{1.63}$$

$$D \doteq A_{RL}^{he} \doteq |t_{he}|^2 \tag{1.64}$$

where the first notation is the one of Ref.[7], and the second notation is in the style of Ref.[8].

Recalling the expression (1.20)-(1.21) and (1.26)-(1.27) for u_0 and v_0 we obtain:

Supra-gap ($E > \Delta_0$)

$$A(E) = A^{he}_{LL}(E) = \frac{\Delta_0^2}{\left(E + (1+2Z^2)\sqrt{E^2-\Delta_0^2}\right)^2} \tag{1.65}$$

$$B(E) = A^{ee}_{LL}(E) = \frac{4Z^2(1+Z^2)(E^2-\Delta_0^2)}{\left(E + (1+2Z^2)\sqrt{E^2-\Delta_0^2}\right)^2} \tag{1.66}$$

$$C(E) = A^{ee}_{RL}(E) = \frac{2(1+Z^2)\sqrt{E^2-\Delta_0^2}\ \ (E+\sqrt{E^2-\Delta_0^2})}{\left(E + (1+2Z^2)\sqrt{E^2-\Delta_0^2}\right)^2} \tag{1.67}$$

$$D(E) = A^{he}_{RL}(E) = \frac{2Z^2\sqrt{E^2-\Delta_0^2}\ \ (E-\sqrt{E^2-\Delta_0^2})}{\left(E + (1+2Z^2)\sqrt{E^2-\Delta_0^2}\right)^2} \tag{1.68}$$

One can easily verify that

$$\sum_{J=L/R}\sum_{\beta=e/h} A^{\beta e}_{JL} = 1 \qquad \Leftrightarrow \qquad A+B+C+D=1 \tag{1.69}$$

as required by unitarity of the S-matrix.

Sub-gap ($E < \Delta_0$)

$$A(E) = A^{he}_{LL} = |r_{he}|^2 = \frac{\Delta_0^2}{E^2 + (1+2Z^2)^2(\Delta_0^2-E^2)} \tag{1.70}$$

$$B(E) = A^{ee}_{LL} = |r_{ee}|^2 = \frac{4Z^2(1+Z^2)(\Delta_0^2-E^2)}{E^2 + (1+2Z^2)^2(\Delta_0^2-E^2)} \tag{1.71}$$

$$C(E) = A^{ee}_{RL} = |t_{ee}|^2 = 0 \tag{1.72}$$

$$D(E) = A^{he}_{RL} = |t_{he}|^2 = 0 \tag{1.73}$$

Notice that in the subgap case the transmission coefficients are vanishing $C = D = 0$. In fact $E = \Delta_0$ is precisely the value at which the supra-gap coefficients (1.67) and (1.81) vanish. For $E < \Delta_0$ one still has a non vanishing analytical continuations for the expressions (1.67) and (1.81). However, they cannot be interpreted as transmission coefficients, for in the superconductor there are no propagating modes for $E > \Delta_0$.

One can again easily verify that

$$\sum_{J=L/R}\sum_{\beta=e/h} A^{\beta e}_{JL} = 1 \qquad \Leftrightarrow \qquad A+B=1 \tag{1.74}$$

as required by unitarity of the S-matrix.

1.7 Andreev Reflection

1.7.1 The case of ideal interface ($Z = 0$)

In order to discuss the physical consequences of the coefficients A, B, C and d found in the previous section, we start by considering the special case of ideal interface ($Z = 0$). In this case the Andreev-reflection amplitude for the process $e \to h$ coefficient reads

$$r_{he} = \frac{v_0}{u_0}\, e^{-i\varphi} = e^{-i\varphi} \begin{cases} e^{-i \arccos \frac{E}{\Delta_0}} & E < \Delta_0 \\ e^{-\mathrm{arccosh} \frac{E}{\Delta_0}} & E > \Delta_0 \end{cases} \tag{1.75}$$

Similarly, one can find for the process $h \to e$ that

$$r_{eh} = \frac{v_0}{u_0}\, e^{i\varphi} = e^{i\varphi} \begin{cases} e^{-i \arccos \frac{E}{\Delta_0}} & E < \Delta_0 \\ e^{-\mathrm{arccosh} \frac{E}{\Delta_0}} & E > \Delta_0 \end{cases} \tag{1.76}$$

The coefficients in this case read:

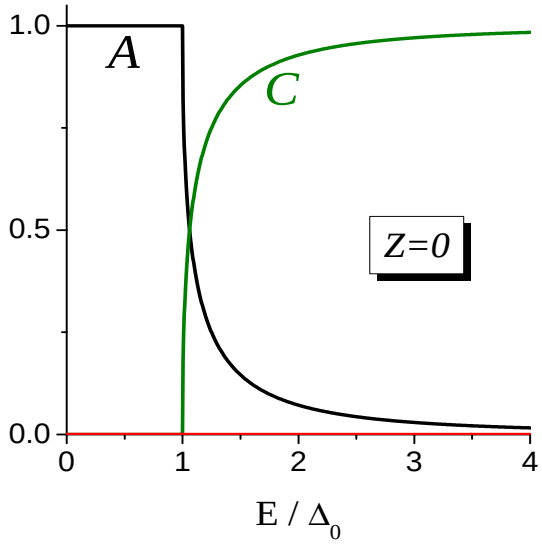

Figure 1.5: The case of ideal interface $Z = 0$: The Coefficients A, and C are plotted as a function of energy. The coefficients B and D are vanishing.

- **Sub-gap regime** ($E < \Delta_0$)

$$A(E) = 1 \tag{1.77}$$
$$B(E) = 0 \tag{1.78}$$
$$C(E) = 0 \tag{1.79}$$
$$D(E) = 0 \tag{1.80}$$

which shows that, for an ideal N-S interface, an injected electron can only be Andreev reflected as a hole, with 100% probability. This phenomenon is known as Andreev reflection[5, 6], and is depicted in Fig.1.6. An incoming electron is reflected as a hole. In contrast to an ordinary reflection, where momentum is not conserved and charge is conserved, in an Andreev reflection process momentum is almost conserved (in the sense that both the incoming electron and the reflected hole have momentum very close to the *same* k_F, whereas charge is not conserved. Importantly, the velocities are reversed.

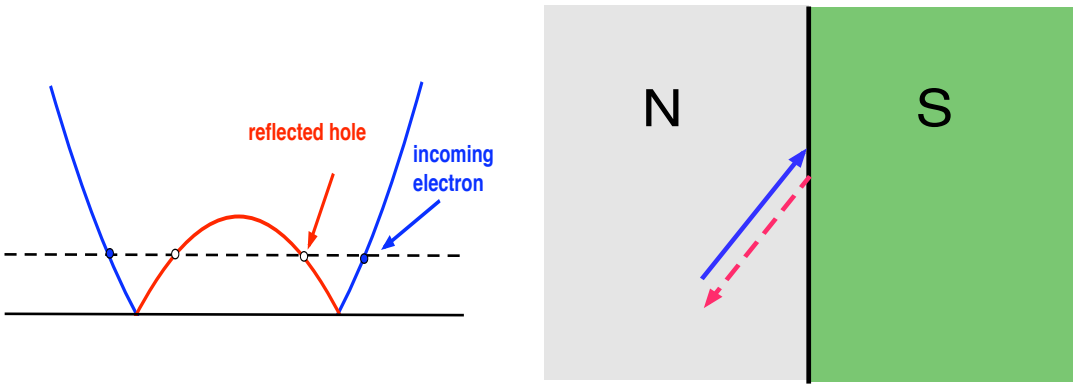

Figure 1.6: The phenomenon of Andreev reflection: the incoming electron is reflected as a hole.

- **Supra-gap regime** ($E > \Delta_0$)

$$A(E) = \frac{\Delta_0^2}{\left(E + \sqrt{E^2 - \Delta_0^2}\right)^2} \tag{1.81}$$
$$B(E) = 0 \tag{1.82}$$
$$C(E) = \frac{2\sqrt{E^2 - \Delta_0^2}}{E + \sqrt{E^2 - \Delta_0^2}} \tag{1.83}$$
$$D(E) = 0 \tag{1.84}$$

Here we see that, for energies above the gap, the electron also has a finite probability to be transmitted as an electron, since single particle states are available in the superconductor above the gap. At high energies $E \gg \Delta_0$, the effects of superconductivity

and normal transmission is in fact the most probable process, as shown by the curve $C(E)$ in Fig.1.5.

1.7.2 Interface with arbitrary transparency

Let us now consider the case of a non-ideal interface ($Z > 0$). There is still a probability that electrons are Andreev-reflected as holes. However, in this situation, due to the presence of the barrier at the interface, electrons can also be ordinarily reflected as electrons. In the sub-gap regime the sum of probabilities of these two processes must equal 1 ($A + B = 1$), so that an increase of ordinary reflection leads to a decrease of Andreev reflection, as shown in Fig.1.7 for two different values of the interface parameter.

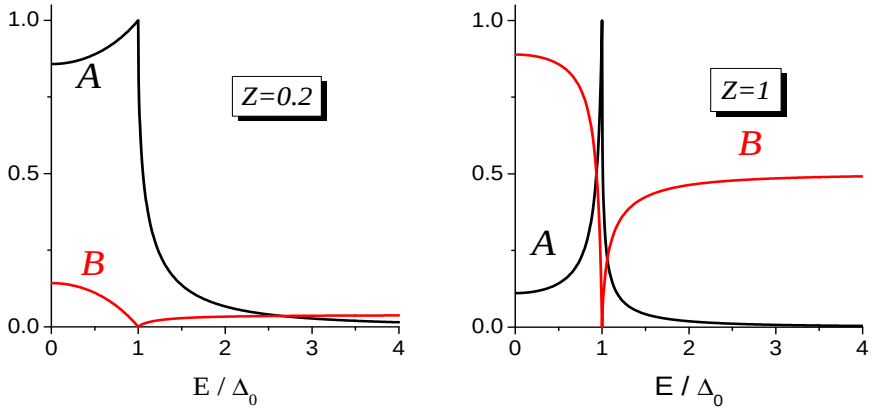

Figure 1.7: The coefficients A and B are plotted as a function of energy for the case of $Z = 0.2$ (almost ideal interface with transmission coefficient $T = 0.96$) and $Z = 1$ (interface with intermediate transmission $T = 0.5$).

Chapter 2

Current-voltage Characteristics

2.1 Current and Conductance

In the case of transport through a system connected to *normal* electrodes, the Landauer-Büttiker expression for the (single channel) current reads

$$I = \frac{2e^2}{h} \int dE \ \underbrace{T(E)}_{=1-R(E)} \ (f_L(E) - f_R(E)) \tag{2.1}$$

where $T(E)$ is the transmission coefficient of the sample, $R(E)$ its reflection coefficient, the pre-factor 2 stems from spin degeneracy, and $f_{L/R}(E)$ the Fermi functions of the Left and Right reservoirs

$$f_X(E) = \frac{1}{1 + e^{(E-\mu_X)/k_B T}} \qquad\qquad X = L/R$$

In the case of a (single channel) mesoscopic sample contacted to one *normal* and one *superconducting* electrode, the formula is modified as follows

$$\boxed{I = \frac{2e^2}{h} \int dE \ (1 - B(E) + A(E)) \ (f_L(E) - f_R(E))} \tag{2.2}$$

where

- $B = |r^{ee}|^2$ is the normal-reflection coefficient and *decreases* the current
- $A = |r^{he}|^2$ is the Andreev-reflection coefficient and *increases* the current

In particular at zero temperature $T = 0$, we have

$$I = \frac{2e^2}{h} \int_0^{eV} dE \ (1 - B(E) + A(E)) \tag{2.3}$$

where we have set

$$\mu_L = \varepsilon_F + eV \qquad\qquad \mu_R = \varepsilon_F \qquad\qquad V > 0$$

The non-linear conductance at zero temperature then reads

$$\boxed{G_{\rm NS}(V) \doteq \frac{dI}{dV} = \frac{2e^2}{h}\left(1 - B(eV) + A(eV)\right)} \tag{2.4}$$

and explicitly

$$G_{\rm NS}(V) = \frac{2e^2}{h}\begin{cases} \dfrac{2\Delta_0^2}{(eV)^2 + (1+2Z^2)^2(\Delta_0^2 - (eV)^2)} & eV < \Delta_0 \\ \dfrac{2eV}{eV + (1+2Z^2)\sqrt{(eV)^2 - \Delta_0^2}} & eV > \Delta_0 \end{cases} \tag{2.5}$$

In particular we notice that

- In the subgap regime $eV \leq \Delta_0$ we have $A + B = 1$ due to unitarity, so that we can also write
$$G_{\rm NS}(V \leq \Delta_0) = \frac{4e^2}{h} A(eV) \tag{2.6}$$
- In the limit of high voltage with respect to the gap ($eV \gg \Delta_0$), superconducting effects become negligible and we obtain the normal conductance (effectively this is equivalent to sending $\Delta_0 \to 0$)
$$G_{\rm NS}(eV \gg \Delta_0) \;\; \to \;\; G_{\rm NN} = \frac{2e^2}{h}\frac{1}{1+Z^2} \tag{2.7}$$
whence we read off the normal transmission coefficient
$$T_N = \frac{1}{1+Z^2} \tag{2.8}$$
of the interface, as anticipated in Eq.(1.60). Equivalently one often denotes by
$$R_N = G_{\rm NN}^{-1} = \frac{h}{2e^2}(1+Z^2) \tag{2.9}$$
the resistance of the normal junction.

The non-linear conductance is plotted at zero temperature in Fig.2.1 for different values of the interface transparency. We observe that

- For high transparency the subpag regime is dominated by Andreev processes ($A \simeq 1$) and therefore $G_{\rm NS}$ is finite, whereas at low transparency Andreev reflection is strongly suppressed in favor of normal reflection, yielding a strong reduction of $G_{\rm NS}(V)$.
- $G_{\rm NS}(V)$ exhibits a cusp at $eV = \Delta_0$, corresponding to the singularity of the density of states of the superconductor at the gap.

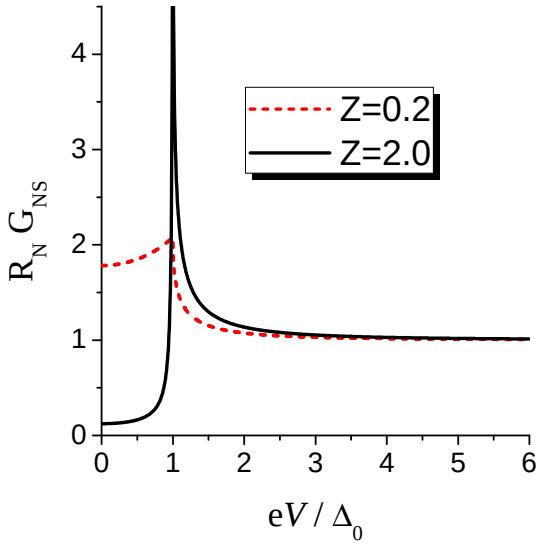

Figure 2.1: The current-voltage characteristics of an N-S junction within the BTK model is plotted at zero temperature and for different values of the barrier strength. The cusp at $eV = \Delta_0$ corresponds to the singularity of the density of states of the superconductor at the gap.

2.1.1 The limit of low transparency at arbitrary V

We can now consider the particular case of a very strong barrier, i.e. a low-transparency interface

$$Z \gg 1 \qquad \Rightarrow \qquad T_N \ll 1 \tag{2.10}$$

and consider the non-linear conductance to lowest order in $\mathcal{O}(1/Z^2)$ (i.e. lowest order in T_N) as a function of V. We obtain from (2.5)

$$G_{\rm NS}(V) = \frac{2e^2}{h} \begin{cases} 0 & eV < \Delta_0 \\ \dfrac{eV}{Z^2\sqrt{(eV)^2 - \Delta_0^2}} & eV > \Delta_0 \end{cases} \tag{2.11}$$

Recalling that to lowest order

$$\frac{2e^2}{h}\frac{1}{Z^2} \simeq \frac{2e^2}{h} T_N = G_{\rm NN} \tag{2.12}$$

and using the definition of density of states for a superconductor

$$N_s(E) = N(0)\frac{E}{\sqrt{E^2 - \Delta_0^2}}\,\theta(E - \Delta_0) \tag{2.13}$$

we can also rewrite that for a low transparency barrier

$$\boxed{G_{\rm NS}(V) = G_{\rm NN}\frac{N_s(eV)}{N(0)} \qquad Z \gg 1} \tag{2.14}$$

2.1.2 The linear conductance at arbitrary transparency

We can now look at the limiting case of the **linear** conductance

$$G_{\rm NS}(0) \doteq \left.\frac{dI}{dV}\right|_{V=0} = \frac{2e^2}{h}\left(1 - B(0) + A(0)\right) \tag{2.15}$$

Recalling that in the subgap regime $B(E) = 1 - A(E)$ because of unitarity, we can also write

$$\boxed{G_{\rm NS}(0) = \frac{4e^2}{h}A(0) = \frac{4e^2}{h}\frac{1}{(1+2Z^2)^2}} \tag{2.16}$$

The linear conductance is thus *twice* the quantum of conductance $2e^2/h$ multiplied by the Andreev reflection coefficient.

One can also re-express the linear conductance in another form, exploiting the normal transmission coefficient derived above.

$$T_N = \frac{1}{1+Z^2} \qquad \Rightarrow \qquad Z^2 = \frac{1-T_N}{T_N}$$

It is indeed straightforward to check that inserting the above expression into Eq.(2.16) one obtains

$$\boxed{G_{\rm NS}(0) = \frac{4e^2}{h}\frac{T_N^2}{(2-T_N)^2}} \tag{2.17}$$

We observe that

- Differently from the the normal conductance

  $$G_{\rm NN}(0) = \frac{2e^2}{h}T_N$$

  the $G_{\rm NS}$ conductance of an N-S junction is a non linear function of the normal transmission coefficient T_N.

- Since $0 \leq T_N \leq 1$ one has the inequality

  $$G_{\rm NS}(0) \leq 2\, G_{\rm NN}(0) \tag{2.18}$$

- At low transparency $T_N \ll 1$, we have that

  $$G_{\rm NS}(0) = \mathcal{O}(T_N^2) \tag{2.19}$$

  i.e. the linear conductance is vanishing to lowest order in the transmission. This is in agreement with the result of the tunneling approach, where one must compute conductance to higher orders in the tunneling amplitudes to obtain non-vanishing contributions.

Bibliography

[1] A. M. Zagoskin, *Quantum Theory of Many-Body System*, Springer Verlag New York (1998).

[2] M. Tinkham, *Introduction to Superconductivity*, Dover Publications, New York (1975).

[3] Y. Blanter and M. Büttiker, *Shot Noise in Mesoscopic Conductors*, [ArXiv version cond-mat/9910158]

[4] C. W. J. Beenakker, in *Transport Phenomena in Mesoscopic Systems* (eds. H. Fukuyama, and T. Ando), Springer Series in Solid State Science **109**, Springer Verlag Heidelberg (1992).

Articles

[5] A. F. Andreev, Sov. Phys. JETP **19**, 1228 (1964).

[6] S. N. Artemenko, A. F. Volkov, and A. V. Zaitsev, JETP Lett. **28**, 589 (1978); Sov. Phys. JETP **49**, 924 (1979); Solid State Comm. **30**, 771 (1979); A. V. Zaitsev, Sov. Phys. JETP **51**, 111 (1980).

[7] G. E. Blonder, M Tinkham, T. M. Klapwijk, Phys. Rev. B **25**, 4515 (1982).

[8] C. J. Lambert and R. Raimondi, J. Phys. Cond. Matt. **10**, 901 (1998); C. J. Lambert, J. Phys Cond. Matt. **3**, 6579 (1991); C. J. Lambert *et al.*, J. Phys. Cond. Matt. **5**, 4187 (1993).

[9] C. W. J. Beenakker, in *Quantum Transport in Semiconductor-Superconductor micro-junctions*, ArXiv cond-mat/9406083